The Thermal Evolution of the Postshock Layer in Pregalactic Clouds

Hajime Susa,[*] Hideya Uehara,[*,**] Ryoichi Nishi[*,***] and Masako Yamada[*,****]

Center for Computational Physics, University of Tsukuba, Tsukuba 305, Japan
*Department of Physics, Kyoto University, Kyoto 606-8502, Japan

We re-examine the thermal evolution of the postshock layer in primordial gas clouds. Comparing the time scales, we find that the evolutionary paths of postshock regions in primordial gas clouds can be basically understood in terms of the diagram drawn in the ionization degree vs temperature plane. The results obtained from the diagram are independent of the density in the case that we do not include photodissociation and photoionization. We also argue that the diagram is not only relevant to the case of the steady postshock flow, but also to the isochorically cooling gas.

§1. Introduction

The thermal evolution of primordial gas clouds has been investigated by many authors.[15),24),3),17),9),20),29)] Almost all of those studies have been concerned with the formation of various kinds of galaxies, or primordial stars. In those papers, galaxies are assumed to grow out of small density perturbations present in the early universe. Because of the coldness of the growing density perturbations, the formed clouds, which are the progenitors of galaxies, experience strong shock heating at the bouncing epoch. Shock heating is also expected in the hierarchical clustering scenario of structure formation. In this case, shocks are expected in the collision between two clouds which are trapped in the gravitational potential well associated with the larger structure.

In any case, shock heating is expected in the era of galaxy formation. The spatial structure and the thermal evolution of the postshock layer in primordial gas clouds were investigated by many authors.[8),26),27),14),23),10),1),30)] In those studies the common and most important point is the over production of hydrogen molecules. For example, in Shapiro and Kang[23)] (hereafter SK), the thermal evolution of steady postshock flow is investigated. They found that the postshock flow cools down so fast that the recombination process cannot catch up with the cooling. As a result, the ionization degree remains high ($y_e \sim 10^{-3}$), even when the temperature has dropped below 10^4 K. Feeded these "relic" electrons, hydrogen molecules form through the processes

---

[*] E-mail: susa@rccp.tsukuba.ac.jp
[**] E-mail: uehara@tap.scphys.kyoto-u.ac.jp
[***] E-mail: nishi@tap.scphys.kyoto-u.ac.jp
[****] E-mail: masako@tap.scphys.kyoto-u.ac.jp

$$H + e \rightarrow H^- + \gamma, \tag{1·1}$$

$$H + H^- \rightarrow H_2 + e. \tag{1·2}$$
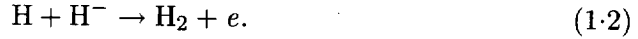
SK stressed the importance of these non-equilibrium cooling processes and the difficulties of describing these processes with a finite-difference scheme.

SK calculated the cases corresponding to the shock velocity in the range (50km/s–300km/s). In all cases, the resulting fractions of hydrogen molecules are $\sim 10^{-3}$, irrespective of the initial shock velocities. Ionization degrees are also independent of the initial shock velocities for the same temperature if $T \ll 10^4$ K. Surprisingly, the convergence is quite good, though chemical equilibrium is not achieved throughout almost the entire evolutionary path. Therefore there may be a clear explanation for the independence of the initial shock velocity.

In this paper we re-examine the thermal evolution of the postshock layer in primordial gas clouds. To elucidate the convergence of the hydrogen molecule fraction in the course of the evolution of the postshock region, we simply compare several important time scales (§2). We find that we can predict the thermal evolution of the postshock layer for any initial conditions in a diagram of the ionization degree versus temperature. In §3 we also test the results obtained in §2 by comparing the results with those of numerical calculations for the steady postshock flow. In §4 we show that the thermal evolution of isochorically cooling gas is very similar to that of steady postshock flow. The remainder of the section is devoted to the further discussion and summary.

§2. Time scales

In this section we compare the time scales which are essential to the thermal evolution of the postshock layer in primordial gas clouds. First of all, we enumerate the definition of the time scales:

$$t_{\text{cool}} \equiv C_{p,v} \frac{\rho k T}{\mu m_p \Lambda}, \tag{2·1}$$

$$t_{\text{ion}} \equiv \frac{n_p}{k^{\text{ion}} n_H n_e} = \frac{1}{k^{\text{ion}} n_N (1 - y_e)}, \tag{2·2}$$

$$t_{\text{rec}} \equiv \frac{n_p}{k^{\text{rec}} n_e n_p} = \frac{1}{k^{\text{rec}} n_N y_e}, \tag{2·3}$$

$$t_{\text{dis}} \equiv \frac{n_{H_2}}{\sum_i k_i^{\text{dis}} n_{H_2} n_i} = \frac{1}{\sum_i k_i^{\text{dis}} n_N y_i}, \tag{2·4}$$

$$t_{\text{for}} \equiv \frac{n_{H_2}}{\sum_{ij} k_{ij}^{\text{for}} n_i n_j} = \frac{y_{H_2}}{\sum_{ij} k_{ij}^{\text{for}} n_N y_i y_j}. \tag{2·5}$$

Here $t_{\text{cool}}, t_{\text{ion}}, t_{\text{rec}}, t_{\text{dis}}$ and t_{for} denote the time scales of cooling, ionization, recombination, H$_2$ dissociation, and H$_2$ formation, respectively.[*] $n_N, n_i, y_i (\equiv n_i/n_N)$,

---

[*] The time scale of thermalization in the postshock layer is shorter than the other time scales. For example, at 2×10^4 K the time scales of thermalization for plasma and neutral gas are about 10^2 and 10^5 times shorter than the ionization time scale, respectively.

k^X, ρ, μ and m_p are the number density of nucleons, the number density of the ith species, the fraction of ith species, the chemical reaction rate coefficient of the "X" process, the mass density, the mean molecular weight, and proton mass, respectively. Λ denotes the net cooling rate which includes radiative and chemical cooling/heating, assuming that the system is optically thin for cooling photons. This assumption is valid for subgalactic clouds with mass $10^6 - 10^8 M_\odot$ and whose densities are smaller than $\sim 10^8$ cm^{-3}. If a cloud violates this condition, the system could be optically thick for the H$_2$ cooling line photons. Another assumption is that the primordial gas does not contain helium but only hydrogen. This assumption affects the mean molecular weight and the cooling rate at high temperature ($T \sim 10^5$ K). However, these are minor effects for the thermal evolution of primordial gas clouds at lower temperature ($T \lesssim 10^4$ K), which we are especially interested in. Therefore, for simplicity we do not include helium. $C_{p,v}$ denotes the heat capacity of the gas cloud. If the gas evolves isobarically, C_p is chosen, and if the cloud is isochoric, C_v is chosen. These quantities are expressed in terms of γ as

$$C_p \equiv \frac{\gamma}{\gamma - 1}, \tag{2.6}$$

$$C_v \equiv \frac{1}{\gamma - 1}, \tag{2.7}$$

where $\gamma = 5/3$ for an ideal gas without molecules. When we are interested in a steady flow, the postshock layer is almost isobaric (see Appendix B).

The ionization time scale (Eq. (2·2)) is defined as the variation time scale of y_e. Another possibility is definition in terms of $1 - y_e$. However, it is not appropriate for the problem we are now interested in, because the magnitude of ionization degree itself is important for the formation of hydrogen molecules. In any case, comparing these five time scales we can find the fastest process without solving detailed time dependent differential equations.

We should remark that *all of these time scales are proportional to ρ^{-1}* if the cooling rate and other reaction rates are proportional to ρ^2. The dominant component of the cooling changes according to the temperature. Below 10^4 K, the H$_2$ line emission dominates the total cooling of the cloud. In this process, the cooling rate is proportional to the number density of the hydrogen molecules at the excited levels whose fraction is proportional to ρ.[7),*)] Hence, the cooling time scale is proportional to ρ^{-1} for $T \lesssim 10^4$ K as in Eq. (2·1). The cooling process in 10^4 K $\lesssim T \lesssim 10^5$ K is dominated by the bound-bound transition of the hydrogen atoms, and the number of the excited hydrogen atoms is determined by collisions with other atoms. Therefore, the cooling rate is proportional to the square of the total density. For higher temperature ($T \gtrsim 10^5$ K), the free-free emission by the collision between ions and electrons dominates the energy radiated away from the cloud. In any case, the cooling rate is proportional to ρ^2, and the cooling time is proportional to ρ^{-1}.[**)]

---

*) This treatment is limited to low density ($n \lesssim 10^4$cm^{-3}). The cooling rate is not proportional to ρ^2 for higher density (higher than the *critical density*).

**) Compton cooling is effective at high redshift and high temperature. In this case, the cooling rate is not proportional to ρ^2, but this does not change the results significantly.

The chemical reaction rates are proportional to ρ^2 if the reactions are dominated by the collisional processes. Photoionization and H_2 photodissociation processes by UV photons emitted from the postshock hot region could affect the ionization rates and the H_2 dissociation rates in the postshock regions. If these radiative reactions dominate the other reactions, total reaction rates will not be proportional to ρ^2, because photoionization and H_2 photodissociation processes are not collisional. Kang and Shapiro [10] investigated this problem. The figures in their paper indicate that the effects caused by the internally produced photons are not too large to dominate that of the collisional processes. Hence, as a 0th-order approximation, we neglect the photoionization and the H_2 photodissociation processes in this paper.

As a result, the ratio of any two time scales is independent of the total density, and they are determined by the temperature and the chemical compositions (y_e and y_{H_2}). As will be discussed later, y_{H_2} is almost always determined by y_e and T. Therefore, the ratio of any two time scales just depends on T and y_e. In the following sections, we compare the time scales individually.

2.1. *Ionization and cooling*

First, we investigate the case $t_{ion} < t_{rec}$, which corresponds to higher temperature ($T \gtrsim 10^4$ K), and we compare the time scale of ionization with that of cooling. As mentioned previously, the ratio t_{ion}/t_{cool} does not depend on ρ, but on the ionization degree y_e and temperature T, because both ionization and cooling, which are dominated by atomic hydrogen line cooling, occur through two-body collisions. Hence the ratio t_{ion}/t_{cool} is determined at each point on the y_e-T plane independently of the density. The line along which t_{ion}/t_{cool} is equal to unity is indicated by the solid line in Fig. 1. If the initial conditions are given below the line, the system is ionized before it cools down, because $t_{ion}/t_{cool} < 1$. Otherwise, the system cools before it is ionized. The expected evolutionary path is also expressed by the arrows in Fig. 1.

2.2. *Recombination and cooling*

Next we investigate the case $t_{rec} < t_{ion}$, which corresponds to lower temperature, and examine the balance between the recombination process and the cooling process. The recombination process is important for $T \lesssim 10^4$ K . When $T \lesssim 10^4$ K, the line cooling of the hydrogen molecules dominates the atomic hydrogen line cooling. Therefore the ratio t_{rec}/t_{cool} depends not only on the ionization degree and the temperature but also on the fraction of hydrogen molecules. In order to draw the line $t_{rec}/t_{cool} = 1$ in the y_e-T plane, we need information on the fraction of hydrogen molecules. As will be discussed in the next subsection, the fraction of H_2 is determined by the chemical equilibrium above $\sim 10^4$ K. Then, it is approximately frozen below $\sim 4 \times 10^3$ K through the evolutionary course with cooling. The line along which $t_{rec}/t_{cool} = 1$ is satisfied is drawn in Fig. 1. In the region above the line, the system recombines before it cools down, and below the line, the system cools down before the recombination proceeds. The expected evolutionary path is also indicated in Fig. 1 by the arrows.
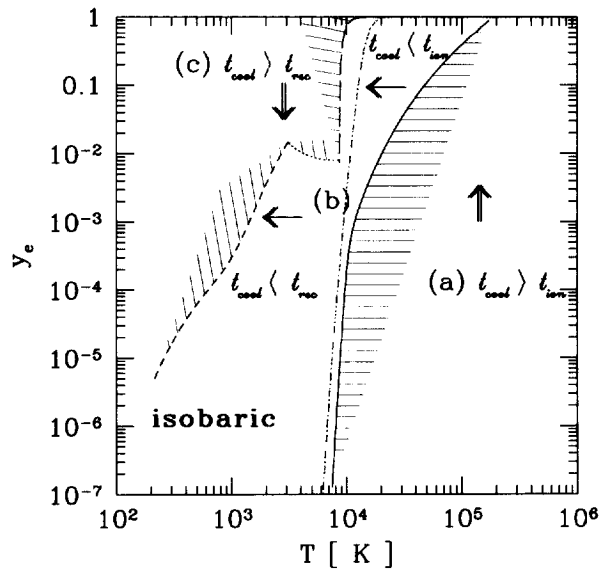
Fig. 1. The y_e-T plane is divided into several regions in which the ratio of the time scales differ. The arrows in the plane denote the directions of the evolution of the postshock layer. The dot–short-dashed curve where the equality $t_{rec} = t_{ion}$ holds. Region (a) in which the condition $t_{ion} < t_{cool}$ holds is bounded by the solid line. In this region, the system evolves upward in the y_e-T diagram. In region (b), the conditions $t_{cool} < t_{ion}$, t_{rec} always hold. Therefore the temperature drops down before the system is further ionized or recombines. In region (c) we have $t_{rec} < t_{cool}$, and the system evolves downward. Region (c) is bounded by the dotted line, short-dashed line and the long-dashed line. Those three lines denote the boundary on which the condition $t_{cool} = t_{rec}$ holds. The long-dashed line was calculated by assuming that the cooling rate is dominated by the hydrogen line cooling. The dotted line was calculated assuming chemical equilibrium of the hydrogen molecules, and the short-dashed line was calculated with $y_{H_2} = 10^{-3}$, which corresponds to the frozen value of the hydrogen molecules for a shock velocity higher than ~ 30 km/s, see also Fig. 2.

2.3. *Fraction of H_2*

Here we investigate whether or not H_2 is in chemical equilibrium. If H_2 is in chemical equilibrium (with given T and y_e), the cooling time is always determined by just T and y_e. As a result, the thermal evolution of the system is completely determined in the y_e-T plane.[*] The fraction of hydrogen molecules is roughly determined by estimating t_{dis} and t_{for}, which denote the time scale of the dissociation and the formation of hydrogen molecules. If at least one of the two time scales is shorter than the other time scales, t_{cool} and t_{rec}, the fraction of hydrogen molecules changes toward the chemical equilibrium value. Hence, the ratios $t_{dis}/t_{cool,rec}$ and $t_{for}/t_{cool,rec}$ should be examined.

First of all, we comment on the important properties of t_{dis} and t_{for}. The time scale of dissociation is independent of y_{H_2}, the fraction of hydrogen molecules. On

---

[*] The other components such as H_2^+ or H^- are always in chemical equilibrium, because they are very fragile.

the other hand, t_{for} is proportional to y_{H_2}. Then both the time scales given in terms of their equilibrium values are

$$t_{\mathrm{dis}} = t_{\mathrm{dis}}^{eq}, \tag{2·8}$$

$$t_{\mathrm{for}} = t_{\mathrm{for}}^{eq} \frac{y_{\mathrm{H}_2}}{y_{\mathrm{H}_2}^{eq}}, \tag{2·9}$$

where the superscript eq denotes the value at which the hydrogen molecules are in chemical equilibrium for a given electron abundance and temperature. Here, the electron abundance is not an equilibrium value in general. Therefore the relation $t_{\mathrm{for}}^{eq} = t_{\mathrm{dis}}^{eq}$ holds.

Suppose that we know the important time scale (t_{sys}) which characterizes the evolution of the system. It could be t_{rec}, t_{cool}, and so on. If t_{sys} is independent of y_{H_2}, we have general arguments as follows: 1) In the case $y_{\mathrm{H}_2} > y_{\mathrm{H}_2}^{eq}$, dissociation proceeds faster than the formation process. Hence, t_{dis} controls the change of y_{H_2}. This is the reason we do not have to be concerned about t_{for}. Since t_{dis} is independent of y_{H_2}, y_{H_2} converges to $y_{\mathrm{H}_2}^{eq}$ if $t_{\mathrm{dis}} < t_{\mathrm{sys}}$ is satisfied. 2) If $y_{\mathrm{H}_2} < y_{\mathrm{H}_2}^{eq}$, y_{H_2} is controlled by the time scale t_{for}, because the system will try to recover the fraction of H_2 which is smaller than the equilibrium value. The maximal value of t_{for} is the equilibrium value, since t_{for} is proportional to y_{H_2}(Eq. (2·9)). Therefore, if $t_{\mathrm{sys}} > t_{\mathrm{for}}^{eq}(= t_{\mathrm{dis}})$, t_{sys} is always greater than t_{for}. As a result, $t_{\mathrm{sys}} > t_{\mathrm{dis}}$ is a sufficient condition for the system to maintain the chemical equilibrium of hydrogen molecules. In the following, we look into the concrete cases that the interesting time scales are t_{rec} and t_{cool}.

2.3.1. $t_{\mathrm{dis,for}}$ vs t_{rec}

First, let us investigate the chemical equilibrium of hydrogen molecules compared to the recombination process. In other words, we investigate the magnitudes of $t_{\mathrm{dis}}/t_{\mathrm{rec}}$ and $t_{\mathrm{for}}/t_{\mathrm{rec}}$. As discussed above, when we compare t_{dis} and t_{for} with other time scales which do not depend on y_{H_2}, we do not have to be concerned about t_{for}. In this case, t_{rec} is independent of y_{H_2}, and hence we only must examine $t_{\mathrm{dis}}/t_{\mathrm{rec}}$. The time scale of recombination, t_{rec} (Eq. (2·3)), is proportional to y_e^{-1}, and the time scale of dissociation is also proportional to y_e^{-1}, because it is governed by collisions between H^+ and H_2. This means that the ratio $t_{\mathrm{dis}}/t_{\mathrm{rec}}$ is independent of y_e. It is also independent of y_{H_2}, and hence the ratio just depends on the temperature. Therefore we have the critical temperature below which $t_{\mathrm{dis}}/t_{\mathrm{rec}}$ is greater than unity (see Fig. 2). This critical temperature is ~ 2600 K. This argument is different if the ionization degree is sufficiently low for the $\mathrm{H} - \mathrm{H}_2$ collision to dominate the $\mathrm{H}^+ - \mathrm{H}_2$ collision. However, within the regions we are interested ($y_e \gtrsim 10^{-5} - 10^{-6}$), the ionization degree is higher than this. The fact that the line $t_{\mathrm{rec}} = t_{\mathrm{dis}}$ is almost vertical in Fig. 2 confirms the validity of this treatment.

2.3.2. $t_{\mathrm{dis,for}}$ vs t_{cool}

Next, we study the chemical equilibrium of H_2 with respect to the cooling of the gas; i.e. we consider the ratio $t_{\mathrm{dis}}/t_{\mathrm{cool}}$ and $t_{\mathrm{for}}/t_{\mathrm{cool}}$. However, we cannot use the previous argument in this case, because the cooling time scale depends on y_{H_2} for $T \lesssim 10^4$ K. Accordingly, we must investigate the individual case again. 1) If $y_{\mathrm{H}_2} < y_{\mathrm{H}_2}^{eq}$, we obtain the relation $t_{\mathrm{for}} < t_{\mathrm{dis}}$. In this case, we do not have to
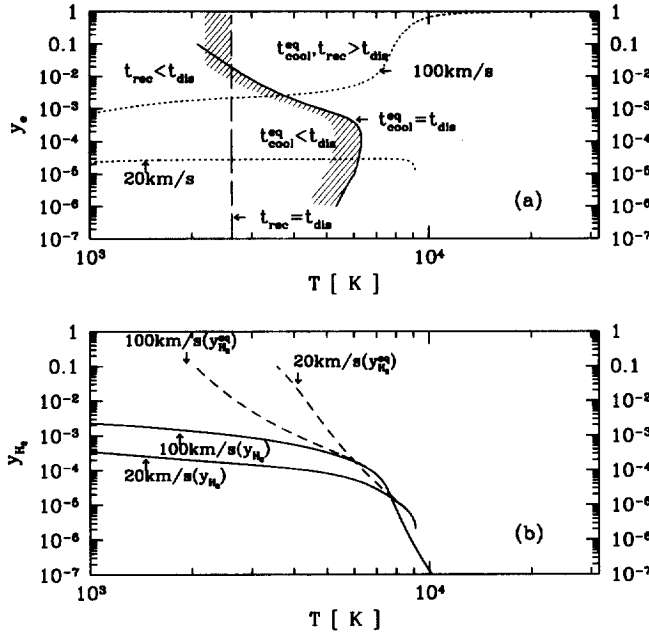
Fig. 2. (a) The y_e-T plane is divided into two regions, where chemical equilibrium is achieved for the fraction of hydrogen molecules and where not. The solid boundary of the shaded region is determined by the condition $t_{\rm cool} = t_{\rm dis}$. The long-dashed line denotes the boundary at which $t_{\rm rec} = t_{\rm dis}$ is satisfied. In the shaded region, the chemical equilibrium of hydrogen molecules breaks down, and the fraction $y_{\rm H_2} \equiv n_{\rm H_2}/n_{\rm H}$ freezes as the temperature and/or ionization degree drops. The dotted lines labeled 100 km/s and 20 km/s denote the evolutionary path of y_e. (b) The equilibrium and the non-equilibrium fraction of hydrogen molecules are drawn in $y_{\rm H_2}$-T plane. The solid lines labeled 100 km/s($y_{\rm H_2}$) and 20 km/s($y_{\rm H_2}$) denote the dynamically calculated evolutionary path of the fraction of hydrogen molecules. The short-dashed lines which are labeled 100 km/s($y_{\rm H_2}^{eq}$) and 20 km/s($y_{\rm H_2}^{eq}$) denote the fraction of H$_2$ calculated assuming the chemical equilibrium of hydrogen molecules with dynamically calculated electron density.

consider $t_{\rm dis}$, because H$_2$ has a smaller fraction than its equilibrium value. The ratio $t_{\rm for}/t_{\rm cool}$ is almost proportional to $y_{\rm H_2}^2$, because $t_{\rm for}$ is proportional to $y_{\rm H_2}$ and $t_{\rm cool}$ is proportional to $y_{\rm H_2}^{-1}$. Therefore the ratio reaches a maximal value at $y_{\rm H_2} = y_{\rm H_2}^{eq}$. This means $t_{\rm for}/t_{\rm cool}$ is always smaller than $t_{\rm for}^{eq}/t_{\rm cool}^{eq}$. Then, if $t_{\rm for}^{eq}/t_{\rm cool}^{eq}$ is smaller than unity, H$_2$ is in equilibrium while the temperature drops. 2) If $y_{\rm H_2} > y_{\rm H_2}^{eq}$, we obtain $t_{\rm for} > t_{\rm dis}$. In this case we just check the ratio $t_{\rm dis}/t_{\rm cool}$, because H$_2$ has larger fraction than its equilibrium value. The ratio $t_{\rm dis}/t_{\rm cool}$ is proportional to $y_{\rm H_2}$. Therefore, the ratio does not reach a maximum at $y_{\rm H_2} = y_{\rm H_2}^{eq}$, but rather a minimum. Then we cannot conclude that $t_{\rm dis}^{eq}/t_{\rm cool}^{eq} < 1$ is a sufficient condition for the chemical equilibrium according to the cooling process. However, in the region $y_{\rm H_2} > y_{\rm H_2}^{eq}$, the fraction of H$_2$ converges to $y_{\rm H_2}^{eq}$ as the system *cools*, because the inclination of the short-dashed lines in Fig. 2(b) (denoting the evolution of $y_{\rm H_2}^{eq}$) is negative. If the inclination is positive, $y_{\rm H_2}$ will depart from the equilibrium value as the temperature drops. In other words, if the hydrogen molecules are not in chemical equilibrium in

the region $y_{H_2} > y_{H_2}^{eq}$, the cooling process proceeds until the system cools down to the state $y_{H_2} = y_{H_2}^{eq}$.

In any case, if the condition $t_{dis}/t_{cool}^{eq} < 1$ is satisfied, the relation $y_{H_2} \simeq y_{H_2}^{eq}$ always holds. In Fig. 2(a) the line on which the condition $t_{dis}/t_{cool}^{eq} = 1$ is satisfied is presented in the y_e-T plane. The shaded region denotes the region in which chemical equilibrium for hydrogen molecules with respect to the cooling or recombination process does not hold. When the system comes into this region, the fraction of hydrogen molecules "freeze". The fraction of hydrogen molecule becomes $\sim 10^{-3}$ if the initial temperature is higher than $\sim 2 \times 10^4$ K. This temperature corresponds to the initial shock velocity, ~ 30 km/s, when we discuss the steady postshock flow. For smaller shock velocities, the initial condition for the chemical compositions is not reset, and the fraction of hydrogen molecule becomes a smaller value.

2.4. *Shock diagram*

In the end of this section, we present a brief summary of §2. The main results of this section are summarized in Fig. 1. The evolution of a shock heated system is basically explained in the y_e-T plane, which we call the "shock diagram"(Fig. 1). The evolutionary path of the postshock layer is obtained by tracing the directions of the arrows in the shock diagram. Postshock gas, which is heated up to high temperature, appears in region (a). In region (a), the shortest time scale is t_{ion} and the system evolves upward and enters region (b). In region (b), t_{cool} is the shortest, and therefore the system evolves leftward this time and comes into region (c). In region (c), t_{rec} is the shortest, and then the system evolves downward, and reenters region (b), where the system evolves leftward again and crosses the boundary of regions (b) and (c). Finally, the system evolves nearly along the short-dashed curve, which is the boundary of regions (b) and (c). For postshock gas which is not heated up to above 2×10^4 K, the thermal evolution is somewhat different from the previous case. In this case, when the system enters region (b) from region (a), the ionization degree is so low that the system does not enter region (c) at $T \simeq 10^4$ K. Then the ionization degree and the fraction of hydrogen molecules do not "forget" the initial conditions of the chemical composition.

2.5. *Convergence of the ionization degree in the steady postshock flow*

The convergences of the ionization degree and the fraction of hydrogen molecules in the steady postshock flow are basically explained by Figs. 1~3. At $T \sim 10^4$ K, the line $t_{rec} = t_{cool}$ becomes nearly vertical, since the dominant cooling process is the hydrogen atomic line cooling which decreases by many orders below $T \sim 2 \times 10^4$ K. If (1) the initial shock velocity is larger than ~ 30 km/s or (2) the initial ionization degree is larger than $\sim 7 \times 10^{-3}$ and the initial temperature is larger than $T \sim 10^4$ K, then the evolutionary path should hit this nearly vertical line (the long-dashed line in Fig. 1). *Because the line $t_{rec} = t_{cool}$ is nearly vertical at $T \simeq 10^4$ K and $y_e \gtrsim 10^{-2}$,* y_e drops to $10^{-3} - 10^{-2}$ without changing the temperature and "forgets" the initial conditions, though y_e is not in chemical equilibrium. The value converged to ($y_e \sim 7 \times 10^{-3}$) is essentially determined by the equation $t_{rec}(y_e, T) = t_{cool}^{eq}(y_e, T)$ at $T \simeq 8000$ K. Here, the temperature (8000 K) is obtained by the equality $t_{rec}/t_{cool}^{Ly\alpha} = 1$,

where $t_{\text{cool}}^{Ly\alpha}$ is the cooling time estimated by the hydrogen line cooling. The equation $t_{\text{rec}}/t_{\text{cool}}^{Ly\alpha} = 1$ depends both on y_e and on T in general, but it depends just on T for $y_e \ll 1$.

The convergence of H_2 is also explained by Fig. 2. According to Fig. 2, H_2 is still in chemical equilibrium just below $T = 10^4$ K, at which temperature the convergence of y_e takes place. As a result, systems which satisfy the previous condition (1) or (2) experience the same state (same y_e, same y_{H_2}) just below $T = 10^4$ K. Therefore y_{H_2} also converges for different initial shock velocities.

§3. Comparison with numerical calculations

In this section we compare the results obtained in the previous section with numerical calculations. The numerical calculations which we performed are the same as that in SK, except that our calculations do not contain helium and the cooling rate due to hydrogen molecules is based on Hollenbach and McKee[7],[*] (see Appendices A and B).

Figure 3 displays the evolution of y_e as a function of the temperature behind the shock front in steady flow. It is obvious that the expected evolutionary path in Fig. 1 agrees very well with the numerically calculated path. We also find that
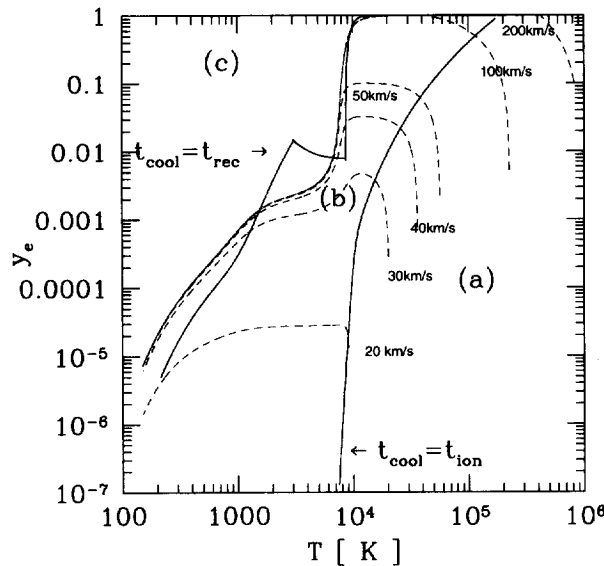

Fig. 3. The evolution of the postshock layer in the y_e-T plane is presented. The solid lines are the boundaries beyond which the direction of the evolution is changed, and each line has the same meaning as in Fig. 1. The short-dashed lines are the numerical results from the SK-type calculation. Each suffix denotes the initial shock velocity.

---

[*] SK used the cooling rate in Lepp and Shull,[12] but their formulae overestimate the cooling rate for lower temperature, $T \lesssim 10^3$ K.
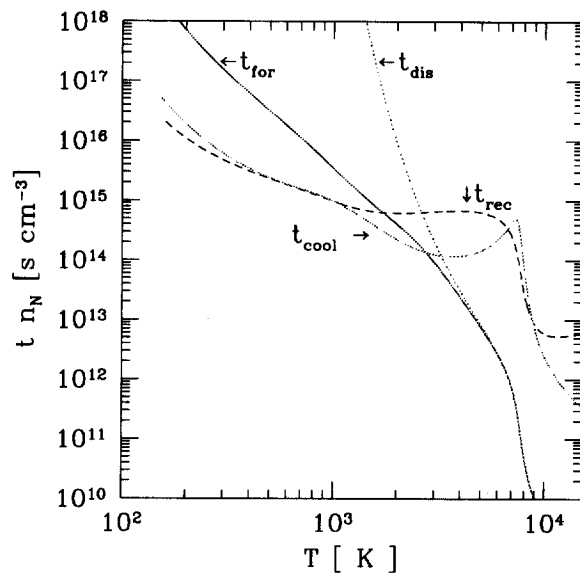
Fig. 4. Evolution of the time scales in the steady flow calculation. The initial shock velocity is 100 km/s. The solid line, dotted line, short-dashed line and long-dashed line represent $t_{\text{for}}, t_{\text{dis}}, t_{\text{rec}}$ and t_{cool}, respectively. Every time scale is multiplied by density.

there exists a critical value of the initial shock velocity above which the evolution of y_e below 10^4 K converges. The critical value of the shock velocity is ~ 30 km/s. This condition for the initial shock velocity is equivalent to condition (1) in the previous subsection. The numerically calculated evolutionary path of y_{H_2} is presented in Fig. 2. The chemical equilibrium for the hydrogen molecule holds outside of the shaded region in the y_e-T plane. Once the system comes into the shaded region, the fraction of H_2 departs from the chemical equilibrium and eventually freezes to a certain value, because the cooling proceeds faster than the dissociation and formation of hydrogen molecules.

The evolution of the time scales in numerical calculation ($v_s = 100$ km/s) is presented in Fig. 4. The dissociation time scale is identical to the formation time scale for $T \gtrsim 4000$ K, and they are smaller than the cooling time. For $T \lesssim 4000$ K, t_{dis} becomes larger than t_{cool}, and y_{H_2} starts to depart from $y_{\text{H}_2}^{eq}$. At a slightly lower temperature, t_{for} also becomes larger than t_{cool}. As a result, the value of y_{H_2} approximately freezes for $T \lesssim 4000$ K. The final value of y_{H_2} is 10^{-3} for $v_s \gtrsim 30$ km/s, and smaller for slower shock velocities. The frozen values degenerate for faster shock velocities, because the ionization degrees also degenerate for $v_s \gtrsim 30$ km/s.

§4. Conclusion and discussion

In this paper, we investigated the thermal evolution of the postshock layer in primordial gas clouds. Because of the delay of the recombination process compared

to *the line cooling due to the hydrogen molecules*, significant amounts of electrons ($y_e \sim 10^{-3}$) remain below 8000 K. Feeded the electrons, H_2 also maintains high abundance ($y_{H_2} \sim 10^{-3}$) for $T \lesssim several \times 10^3$ K, then the cloud temperature drops to $T \sim 100$ K quickly due to the H_2 line cooling. We have shown that both of the residual values of y_e and y_{H_2} are universal for $v_s \gtrsim 30$ km/s by simple comparison of time scales. The universality of the values to which y_e and y_{H_2} converge is explained as follows: The evolution of the system is basically determined by T, y_e and y_{H_2}. However, at high temperature, y_{H_2} attains its equilibrium value, and at low temperature, it will freeze to a value, because cooling precedes the dissociation and the formation of hydrogen molecules. Therefore the evolution of the system is predicted just by T and y_e. The convergence of y_e and y_{H_2} occurs when the coolant changes from hydrogen atoms to hydrogen molecules. In fact, assuming an isobaric cooling time, the predicted evolutionary paths agree very well with the numerically integrated paths for steady flow.

These results are not restricted to the case of steady postshock flow, and what is more, the shock diagram describes not only the evolution of the postshock flow but also the primordial gas cloud which is once heated up to 10^4 K. The argument in §2 simply depends on the comparison of time scales. When we compare the shock diagram (Fig. 1) with the numerically integrated results, the steadiness of the flow is used just as the isobaricity of the postshock flow in Eq. (2·1), by choosing C_p. However, even if we choose C_v in Eq. (2·1), $t_{\rm cool}$ is not much different from the cooling time for the isobaric flow. We have

$$\frac{t_{\rm cool}^{\rm isobaric}}{t_{\rm cool}^{\rm isochoric}} = C_p/C_v, \qquad (4·1)$$

$$= \gamma. \qquad (4·2)$$

Consequently, the y_e-T diagram obtained for the isochoric case is very similar to Fig. 1. The diagram for the isochoric case is presented in Fig. 5. It is obvious that the difference between Fig. 1 and Fig. 5 is small. In the isochoric case, the final fraction of hydrogen molecules is $\sim 10^{-3}$ again, as in the isobaric case. Hence, the intermediate case should have a similar diagram. Furthermore, the shock diagrams are applied not only to the postshock flow but also to primordial gas clouds which are initially sufficiently heated ($T \gtrsim 10^4$ K).

Hence the argument in the previous paragraph implies that the thermal evolution of the primordial gas cloud is determined by the "shock diagram", unless the system becomes gravitationally unstable or some processes originating from external radiation fields become important. The dynamical evolution of the system is roughly determined by the sound crossing time $t_{\rm sc}$, free-fall time $t_{\rm ff}$, and $t_{\rm cool}$. In the case that $t_{\rm sc}$ is the shortest time scale, the evolution of the system is nearly isobaric, and in the case that $t_{\rm cool}$ is the shortest, the evolution is approximately isochoric. In both cases, we can apply the shock diagrams on the thermal evolution of the system. In the third case, when $t_{\rm ff}$ is the shortest, the evolution is different from both of the above two cases. However, in a realistic situation, such as the shocks in dynamically collapsing primordial gas clouds, at first the isobaric case is realized generally, as discussed by Yamada and Nishi.[30] Results of numerical simulations also imply that
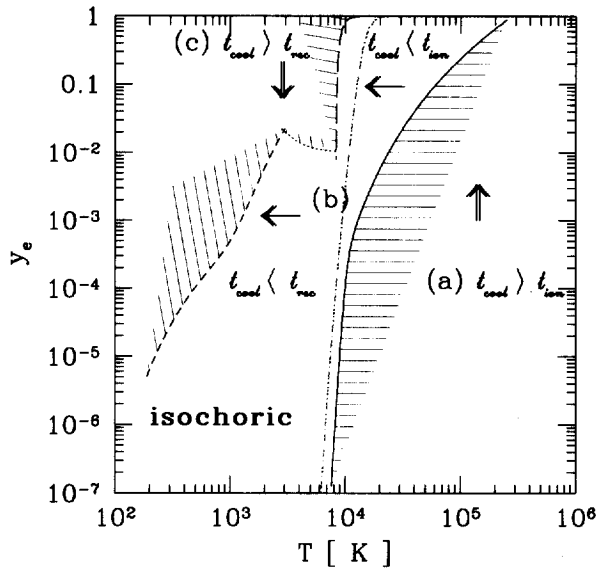
Fig. 5. Same as Fig. 1, except that the cooling time is estimated by assuming the isochoric evolution of the cloud.

the shock diagrams can be applied in this situation. In fact, in dynamically collapsing primordial gas clouds, hydrogen molecules are formed up to $y_{H_2} \sim 10^{-3}$,[1),28)] though the gas is not always isobaric because of a non-steady state of the shock wave.

The gravitational instability of sheets may change the thermal evolution of the primordial gas from the predicted path in the shock diagram. The shocked and compressed layer may fragment into small pieces with a roughly *local* free-fall time which is proportional to $\rho^{-1/2}$ (Ref. 6)). In steady shock waves, Yamada and Nishi[30)] discussed this problem by comparing the time scale of fragmentation and the cooling time.

The external UV radiation field, which exists at the early epoch of the universe, may affect the thermal evolution of pregalactic gas. The reaction rates of photoionization process and photodissociation process have different dependence on density from the other reactions induced by collision. As a result, the above arguments based on Figs. 1 and 5 are changed significantly. However, the external UV radiation field does not exist, as long as we are interested in the first objects in the universe.

Consequently, once the primordial gas cloud is heated above 10^4 K and there is no external radiation field, significant amounts of hydrogen molecules are formed ($y_{H_2} \sim 10^{-3}$), and the temperature drops much below 10^4 K, until some other time scales become comparable to the thermal and chemical time scales.

Acknowledgements

Appendix A
—— *Reactions* ——

We include the following reactions to obtain the dynamical evolution of the postshock layer in §3. The reaction rates are given in the listed reference in Table I.

Table I. Reaction rates.

Reactions	References
$H^+ + e \rightarrow H + \gamma$	Spitzer 1956 [25]
$H + e \rightarrow H^- + \gamma$	de Jong 1972 [4]
$H^- + H \rightarrow H_2 + e$	Beiniek 1980 [2]
$3H \rightarrow H_2 + H$	Palla, Salpeter and Stahler 1983 [17]
$H_2 + H \rightarrow 3H$	SK [23]
$2H + H_2 \rightarrow 2H_2$	Palla, Salpeter and Stahler 1983 [17]
$2H_2 \rightarrow 2H + H_2$	SK [23]
$H + e \rightarrow H^+ + 2e$	Lotz 1968 [13]
$2H \rightarrow H + H^+ + e$	Palla, Salpeter and Stahler 1983 [17]
$H + H^+ \rightarrow H_2^+ + \gamma$	Ramaker and Peek 1976 [21]
$H_2^+ + H \rightarrow H_2 + H^+$	Karpas, Anicich and Huntress 1979 [11]
$H_2 + H^+ \rightarrow H_2^+ + H$	Prasad and Huntress 1980 [19]
$H^- + H^+ \rightarrow H_2^+ + e$	Poularert et al. 1978 [18]
$H_2^+ + e \rightarrow 2H$	Mitchell and Deveau 1983 [16]
$H_2^+ + H^- \rightarrow H + H_2$	Prasad and Huntress 1980 [19]
$H^- + e \rightarrow H + 2e$	Duley 1984 [5]
$H^- + H \rightarrow 2H + e$	Izotov and Kolensnik 1984 [8]
$H^- + H^+ \rightarrow 2H$	Duley 1984 [5]

Appendix B
—— *Steady Shock* ——

In this appendix, the basic equations of the steady shock are presented. The numerical results presented in §3 are based on the following equations. SK solved these equations coupled with the chemical reactions. One of the most important features of the steady shock is the approximate isobaricity of the postshock layer.

B.1. *Basic equations*

The jump conditions at the shock front are

$$\rho_1 v_1 = \rho_2 v_2, \tag{B·1}$$

$$\rho_1 v_1^2 + p_1 = \rho_2 v_2^2 + p_2, \tag{B·2}$$

$$v_1\left(\frac{\rho_1 v_1^2}{2} + \frac{\gamma_1}{\gamma_1 - 1}p_1\right) = u_2\left(\frac{\rho_2 v_2^2}{2} + \frac{\gamma_2}{\gamma_2 - 1}p_2\right). \tag{B·3}$$

These equations constitute the conservation law of the mass, momentum and energy across the shock front. The quantities whose suffixes are 1 and 2 denote the hydrodynamical variable in the preshock region and the postshock region, respectively. In case that the shock is strong, i.e. the sound velocity in the preshock region is much smaller than the bulk velocity u_1, we obtain from Eqs. (B·1) $\sim$ (B·3),

$$\rho_2/\rho_1 = v_1/v_2 = 4, \tag{B·4}$$

$$kT = \frac{3}{16}\mu m_p v_1^2, \tag{B·5}$$

where μ and m_p are the mean molecular weight of the gas and proton mass.

Behind the shock front, the assumption that the flow is steady allows us to write the conservation of mass, momentum and the energy as

$$\rho v = \rho_2 v_2, \tag{B·6}$$

$$\rho v^2 + p = \rho_2 v_2^2 + p_2, \tag{B·7}$$

$$\frac{dE}{dt} = (\Gamma - \Lambda) + [(p + E)]\frac{1}{\rho}\frac{d\rho}{dt}, \tag{B·8}$$

where Γ, Λ and E denote the heating and cooling rates, and the internal energy per unit volume, and d/dt is the Lagrange derivative. The hydrodynamical variables with no suffix denote quantities at a general point behind the shock front. In addition, we require the equation of state $p = nkT$. Then the equations are closed, and we can solve the flow equations.

B.2. *Isobaricity of the postshock layer*

The assumption that the flow is steady indicates the approximate isobaricity of the postshock region (Ref. 30)). From Eqs. (B·7) and (B·8) and the equation of state, $p = \rho kT/(m_p\mu)$, the relative compression factor $x \equiv \rho/\rho_2$ is given by

$$\frac{kT}{m_p\mu}x^2 - \left(1 + \frac{p_2}{\rho_2 v_2^2}\right)x + v_2^2 = 0. \tag{B·9}$$

In case the shock is strong, the above equation becomes

$$\frac{kT}{m_p\mu}x^2 - 4v_2^2 x + v_2^2 = 0. \tag{B·10}$$

Its solution exists if the condition

$$v_2^2\left(4v_2^2 - \frac{kT}{m_p\mu}\right) \geq 0 \tag{B·11}$$

is satisfied, and this condition holds unless the heating rate is not too high to raise the temperature by a factor of 4/3 in the postshock flow.

The solution is expressed as

$$x = \frac{m_p \mu}{kT} v_2^2 \left(2 + \sqrt{4 - \frac{kT}{m_p \mu v_2^2}} \right). \tag{B·12}$$

If we define T_2 as

$$kT_2 = 3\mu m_p v_2^2, \tag{B·13}$$

the pressure p can be written as follows:

$$p = \frac{2}{3} p_2 \left(1 + \sqrt{1 - \frac{3}{4} \frac{T}{T_2}} \right). \tag{B·14}$$

Thus, p/p_2 can be determined by T/T_2 only, and the dependence is weak.

After the gas has cooled down to $T \ll T_2$, p has the asymptotic value, $4/3 p_2$, which is not much different from p_2. As a result, the postshock region is almost isobaric for a wide range of temperatures.

References

1) P. Anninos and M. J. Norman, Astrophys. J. **460** (1996), 556.
2) R. J. Beiniek, J. of Phys. **B13** (1980), 4405.
3) R. G. Carlberg, Mon. Not R. Astron. Soc. **197** (1981), 1021.
4) T. de Jong, Astron and Astrophys. **20** (1972), 263.
5) W. W. Duley and D. A. Williams, *Interstellar Chemistry* (Academic Press, London, 1984).
6) B. G. Elmegreen and D. M. Elmegreen, Astrophys. J. **220** (1978), 1051.
7) D. Hollenbach and C. McKee, Astrophys. J. Suppl. **41** (1979), 55.
8) Yu. I. Izotov and I. G. Kolensnik, Sov. Astron. **28** (1984), No. 1, 15.
9) O. Lahav, Mon. Not R. Astron. Soc. **220** (1986), 259.
10) H. Kang and P. R. Shapiro, Astrophys. J. **386** (1992), 432.
11) Z. Karpas, V. Anicich and W. T. Huntress, Jr., J. Chem. Phys. **70** (1979), No. 6, 2877.
12) S. Lepp and J. M. Shull, Astrophys. J. **270** (1983), 578.
13) W. Lotz, Z. Phys. **216** (1968), 241.
14) M. M. MacLow and J. M. Shull, Astrophys. J. **302** (1986), 585.
15) T. Matsuda, H. Sato and H. Takeda, Prog. Theor. Phys. **42** (1969), 219.
16) G. F. Mitchell and T. J. Deveau, Astrophys. J. **266** (1983), 646.
17) F. Palla, E. E. Salpeter and S. W. Stahler, Astrophys. J. **271** (1983), 632.
18) G. Poularert, F. Brouillard, W. Claeys, J. W. McGowan and G. Van Wassenhove, J. of Phys. **B11** (1978), L671.
19) S. S. Prasad and W. T. Huntress, Jr., Astrophys. J. Suppl. **43** (1980), 1.
20) D. Puy and M. Signore, Astron and Astrophys. **305** (1996), 371.
21) D. E. Ramaker and J. M. Peek, Phys. Rev. **A13** (1976), 58.
22) M. J. Rees and J. P. Ostriker, Mon. Not R. Astron. Soc. **179** (1977), 541.
23) P. R. Shapiro and H. Kang, Astrophys. J. **318** (1987), 32.
24) J. Silk, Astrophys. J. **214** (1977), 152.
25) L. Spitzer, Jr., *The Physics of Fully Ionized Gases* (Interscience, New York, 1956), p. 88.
26) C. Struck-Marcell, Astrophys. J. **259** (1982), 116.
27) C. Struck-Marcell, Astrophys. J. **259** (1982), 127.
28) H. Susa, Thesis "The thermal evolution of primordial gas clouds: A clue to galaxy formation", Kyoto University, Japan, 1997.
29) H. Susa, H. Uehara and R. Nishi, Prog. Theor. Phys. **96** (1996), 1073.
30) M. Yamada and R. Nishi, submitted to Astrophys. J. (1997).